Particle-in-cell simulations of the runaway breakdown of nitrogen

D. Levko and Ya. E. Krasik
Physics Department, Technion, Haifa 32000, Israel

(Received 9 October 2012; accepted 13 November 2012; published online 14 December 2012)

The runaway breakdown initiated by a mono-energetic beam of runaway electrons propagating through a cathode-anode gap filled with nitrogen at atmospheric pressure is studied using the one-dimensional particle-in-cell numerical model. It is shown that the breakdown is strongly influenced by the amplitude of the beam, its duration, and the electric field in the vicinity of the cathode. In addition, the simulation results showed that, in spite of the formation of rather dense plasma inside the cathode-anode gap by runaway electrons, the electric field is not screened because of frequent electron–neutral collisions. © *2012 American Institute of Physics*. [http://dx.doi.org/10.1063/1.4769748]

I. INTRODUCTION

In 1992, Gurevich *et al.*[1] considered the phenomenon of runaway breakdown, which was demonstrated later in laboratory experiments.[2,3] The physical essence of the mechanism of runaway breakdown is related to the Coulomb character of the cross section of a collision between high-energy electrons (1–10 keV) and neutral molecules: the cross section drops as $1/\varepsilon_e^2$ for energetic electrons. Therefore, if the energy of an electron exceeds some critical value ε_{cr} and this electron propagates in an electric field also exceeding some critical value, E_{cr}, corresponding to ε_{cr}, it gains more energy along one mean free path as compared with what it would lose in inelastic collisions. Such electrons are called runaway electrons (RAE). Critical energy ε_{cr} and critical electric field E_{cr} are related by[4]

$$\varepsilon_{cr} \cdot [a/\ln(2\varepsilon_{cr}/I)] = E_c m_e c^2/E_{cr}. \quad (1)$$

Here m_e is the mass of the electron, I is the average energy of inelastic losses along one mean free path equal to 80 eV in nitrogen, $a = 11$ is the constant, c is the speed of light, and $E_c = 2.16 \times 10^3$ V/cm. Using Eq. (1), one obtains that all electrons having energies $\varepsilon_e > 40$ eV and moving in $E_{cr} \approx 4.5 \times 10^5$ V/cm become RAE. If the energy of electrons' ε_{cr} increases, the value of E_{cr} decreases.

Today, there is no doubt that RAE play a crucial role in high-voltage pulsed nanosecond discharges,[5–7] pre-ionizing the cathode-anode (CA) gap, and making it conductive. The role of RAE in high-voltage nanosecond discharges was confirmed by the both experimental (see, for instance, Refs. 5–10) and numerical (see, for instance, Refs. 11–17) studies. In Ref. 11, the hydrodynamic modeling of nanosecond discharge was carried out, while the particle-in-cell (PIC) simulations in one and three dimensions were carried out in Refs. 12–17.

The highly non-uniform electric field is typical for high-voltage nanosecond discharges. Its value in the vicinity of the cathode can greatly exceed the E_{cr} necessary for thermal electrons to become RAE (in nitrogen $E_{cr} \approx 4.5 \times 10^5$ V/cm for thermal electrons). Therefore, the majority of field emitted electrons become RAE. At larger distances from the cathode, one has $E_1 < E_{cr}$ for thermal electrons, and secondary electrons generated in ionization events cannot become RAE. However, RAE that were generated in the vicinity of the cathode have $\varepsilon_e > \varepsilon_{cr}$, and for these electrons, the condition $E_1 > E_{cr}$ is satisfied, i.e., a situation similar to runaway breakdown occurs. This idea was used by Gurevich *et al.*[3] to demonstrate the runaway breakdown in laboratory conditions. It was obtained that the breakdown was initiated by a picosecond electron beam, that is, the breakdown occurred only when electrons with energy exceeding the energy threshold for the development of a runaway breakdown were present in the gap.

Kutsyk *et al.*[18] carried out numerical simulations using the PIC code ELIZA to explain the experimental results of Gurevich.[3] The main purpose of these simulations was to explain two peaks in the RAE flow through the anode, which were separated in time by an interval of several tens of picoseconds. It was supposed that the mono-energetic beam of the RAE with an initial energy of 10 keV and width at the half maximum of 70 ps is injected into the CA gap. Only the electrons with $\varepsilon_e \geq 1$ keV were considered in these simulations, and therefore, the authors were not able to study the runaway breakdown in detail since the majority of secondary electrons have $\varepsilon_e \ll 1$ keV. Simulations showed that the avalanche of RAE generated in ionization events is negligibly small as compared with the primary beam. Therefore, the authors[18] concluded that the second peak cannot be associated with RAE generated from the secondary electrons. An alternative mechanism was proposed for the generation of these secondary RAE, namely, their generation between the plasma approaching the anode and the anode.

This work presents the results of numerical simulations of the runaway breakdown in a CA gap filled with N_2 gas at atmospheric pressure depending on the parameters of the injected RAE beam.

II. NUMERICAL MODEL

In order to study the RAE breakdown, the one dimensional PIC numerical code developed in Ref. 17 to study high-voltage nanosecond discharges in gases was modified. A coaxial diode filled with N_2 gas at 10^5 Pa pressure and with a cathode and anode radius of $R_C = 3$–300 μm and 1 cm, respectively, and a length of 1 cm was considered. Briefly, the sequence of the 1D PIC simulation was as follows:

(a) Solution of the Poisson equation at the beginning of each time step for new electron and ion space charge densities and for fixed boundary conditions, zero anode potential and constant cathode potential $-\varphi_C$; (b) injection of RAE, whose number was defined by the parameters of the beam (temporal duration τ and amplitude N_{max}); all RAE have fixed constant energy 10 keV; it was supposed that the RAE beam has a temporal duration of $\tau = 70$-100 ps with a total number of 10^9-10^{11} electrons, which corresponds to experimentally obtained data (see, for instance, Refs. 5–7); (c) analysis of electron elastic and inelastic collisions[19] (ionization, ionization of *K*-shell, bremsstrahlung, and excitation of the electron levels $A^3\Sigma_u^+$ and $C^3\Pi_u$) using the Monte-Carlo method. In addition, electron scattering forward and backward was considered as well; (d) particles weighting on the spatial grid and returning to step (a). A time step of 10^{-14} s allows us to consider electrons propagating along only a part of the mean free path during one time step. All electrons generated in ionization events had zero energy. The energy of ejected electron according to Ref. 20 can be defined as

$$\varepsilon_{eject} = B \cdot \tan\left(rnd \cdot \arctan\left(\frac{\varepsilon_0 - \varepsilon_{ion}}{2B}\right)\right),$$

where *rnd* is the random number, ε_0 is the energy of primary electron, ε_{ion} is the ionization potential, and B is the constant. Assuming $B = 10$ and $\varepsilon_0 = 10$ keV, one will obtain that less than 5% of ejected electrons have energy exceeding 100 eV. Considering that electrons are generated in a decreasing electric field, one can neglect the possibility of RAE generation in ionization events.

III. RESULTS AND DISCUSSION

Simulations showed that the electric field in the vicinity of the cathode influences significantly the propagation of the RAE beam through the CA gap filled with pressurized gas and the runaway breakdown. Fig. 1 presents a comparison

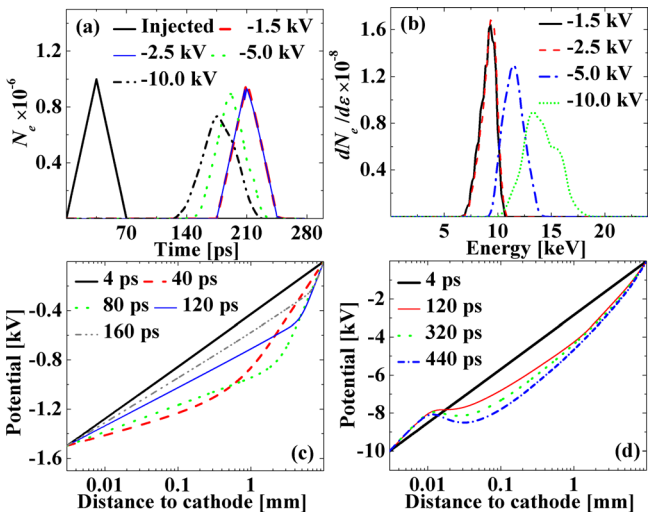

FIG. 1. (a) Temporal evolution of the RAE beam injected into the CA gap and reaching the anode at different cathode potentials; (b) electron energy distribution function at the anode at different cathode potentials; (c) and (d) potential distributions in the CA gap at different times at $|\varphi_C| = 1.5$ kV and $|\varphi_C| = 10$ kV, respectively. $R_C = 3$ μm, $\tau = 70$ ps, and $N_{max} = 10^6$.

between the results of the simulations of the electron beam time evolution and the electron energy distributions at the anode and the potential distributions obtained at different cathode potentials. The value of the electric field in the vicinity of the cathode is $E_{cath} \approx 6 \times 10^5$ V/cm at $|\varphi_C| = 1.5$ kV, $E_{cath} \approx 10^6$ V/cm at $|\varphi_C| = 2.5$ kV, $E_{cath} \approx 2 \times 10^6$ V/cm at $|\varphi_C| = 5$ kV, and $E_{cath} \approx 4 \times 10^6$ V/cm at $|\varphi_C| = 10$ kV, i.e., $E_{cath} > E_{cr}$ in all cases. The electric field already decreases to a value $E < E_{cr}$ at distances of 4 μm, 6.6 μm, 13 μm, and 27 μm at cathode potentials of 1.5 kV, 2.5 kV, 5 kV, and 10 kV, respectively. Taking into account that the mean free path of electrons with $\varepsilon_e = 10$ keV is $\lambda \approx 30$ μm, one can conclude that the major part of the electrons at $|\varphi_C| \leq 5$ kV is generated in $E < E_{cr}$ and there is no input to RAE by secondary electrons that appear as a result of gas ionization. At $|\varphi_C| = 10$ kV, a small fraction of secondary electrons are produced in the region with $E > E_{cr}$; these electrons become RAE with energy $\varepsilon_e < 5$ keV, and their fraction with respect to the total number of RAE that reached the anode is ≈10%. Nevertheless, secondary electrons play an important role in discharge dynamics, since their mean free path is significantly smaller than that of electrons with $\varepsilon_e = 10$ keV.

Fig. 1(a) shows the temporal spread of an RAE beam injected into the CA gap and reaching the anode at different values of the cathode potential. One can see the spread of the beam and the decrease in its amplitude at larger values of $|\varphi_C|$. This spread is caused by the generation of RAE from secondary electrons ($\varepsilon_e < 5$ keV), which reach the anode with a time delay with the respect to RAE having $\varepsilon_e > 10$ keV. The spread of the electron energy distribution function (EEDF) [see Fig. 1(b)] at the anode at values of $|\varphi_C|$ of 1.5 kV, 2.5 kV, and 5 kV is caused by two factors. On the one hand, electrons from the head of the RAE beam are accelerated in the electric field and gain additional energy almost equal to $e\varphi_C$. On the other hand, the space charge of these electrons is large enough to disturb the external electric field [see Fig. 1(c), snapshots for time of 40 ps and 80 ps] and to decelerate the electrons from the tail of the RAE beam. In addition, this disturbed electric field in the vicinity of the cathode is revealed to be smaller than E_{cr}, and secondary electrons cannot become RAE. It is important to note that the density of the plasma generated during the RAE beam propagation through the CA gap reaches $n_e \approx 5.6 \times 10^{14}$ cm^{-3} at $|\varphi_C| = 1.5$ kV and $n_e \approx 3.8 \times 10^{14}$ cm^{-3} at $|\varphi_C| = 5$ kV, i.e., the plasma density decreases with the increase in the cathode potential.

The results of the simulations showed that the most energetic electron beam at the anode is obtained at $|\varphi_C| = 5$ kV [see Fig. 1(b)]. The mean free path of these electrons is larger than that of electrons propagating through the CA gap with $|\varphi_C| = 1.5$ kV. Therefore, the more energetic RAE beam obtained at $|\varphi_C| = 5$ kV generates less dense plasma. Let us note that, in spite of the plasma density being $>10^{14}$ cm^{-3} for both the considered cathode potentials, one does not obtain a significant disturbance of the external field when the electron beam reaches the anode. This can be explained by the dominant role of electron-neutral collisions determining the plasma resistivity, which remains large

enough to allow the external electric field to remain inside the plasma.

A rather different dynamics of the discharge is obtained at $|\varphi_C| = 10\,\text{kV}$. In this case, the space charge of RAE beam affects the external electric field a little, which results in the electric field in the vicinity of the cathode $E_{cath} > E_{cr}$. Thus, secondary electrons generated in the vicinity of the cathode become RAE leaving an uncompensated positive charge in that region, which leads to an additional increase in the value of E_{cath} [see Fig. 1(d)]. In addition, the results of the simulations showed that, in spite of more energetic RAE propagating through the CA gap, the density of the plasma generated at $|\varphi_C| = 10\,\text{kV}$ is larger than those at $|\varphi_C| = 1.5\,\text{kV}$ ($1.8 \times 10^{15}\,\text{cm}^{-3}$ versus $5.6 \times 10^{14}\,\text{cm}^{-3}$). This result indicates the importance of the secondary electrons that are generated in the vicinity of the cathode. These secondary electrons become RAE with $\varepsilon_e < 10\,\text{keV}$ with a mean free path smaller than that of primary RAE, having $\varepsilon_e > 10\,\text{keV}$. Therefore, these secondary electrons ionize and excite N_2 more efficiently than the primary RAE. The high rate of excitation of N_2 molecules makes it possible to observe the fast ionization wave (FIW) propagating toward the anode (see Ref. 22). In a recent study[23] of RAE generation with N_2 gas where $E \sim 10^7\,\text{V/cm}$, the velocity of FIW calculated using the change of concentration of excited $N_2(C^3\Pi_u)$ in space and time reached $\sim 10^9\,\text{cm/s}$. In the present simulations, this velocity is $\sim 1.6 \times 10^6\,\text{cm/s}$ at $\tau = 70$ ps, $|\varphi_C| = 10\,\text{kV}$, and $N_{max} = 10^6$, which is significantly smaller than the velocity of FIW typical for nanosecond high-voltage discharges. Finally, for the case $|\varphi_C| = 10\,\text{kV}$, the comparison between Fig. 1(a) and Fig. 1(d) shows that the electric field remains disturbed after the RAE beam leaves the CA gap. This can be explained by a large electric field causing the separation between movable electrons and immovable ions in the vicinity of the cathode in the considered time scale. Let us define the location where this space charge separation occurs as a streamer propagating towards the anode. The results of the simulations showed that the velocity of the streamer is $\sim 7.3 \times 10^6\,\text{cm/s}$, which agrees well with the typical values of streamer propagation in pressurized gases.[21] It is important to note that the transition from diffuse to spark discharge during one high-voltage nanosecond pulse shot was obtained in recent experiments carried out by Shao *et al.*[8–10] This transition could be explained using results presented in this paper. The diffuse mode could be explained by the pre-ionization of the CA gap by the RAE and formation of a low-ionized and relatively high resistivity plasma. Later, when these RAE leave the CA gap, one obtains the streamer formation in the vicinity of the cathode according to described mechanism.

The results of the simulations showed that the increase in the duration (50–100 ps) of the RAE beam that was injected into the CA gap with a constant value of N_{max} during its propagation toward the anode does not change the evolution of the runaway breakdown significantly. On the contrary, the increase in the value of N_{max} changes drastically both the RAE beam propagation and discharge dynamics (see Fig. 2). The temporal and energy spreads of the RAE beam at $N_{max} = 10^7$ are shown in Figs. 2(a) and 2(b), respectively. Fig. 2(c) shows that the space charge of RAE is large enough to disturb the external electric field significantly. One can see that the potential inside the CA gap reaches $|\varphi| \approx 9\,\text{kV}$, which is smaller than injected electron energy but larger than $|\varphi_C| = 1.5\,\text{kV}$. Therefore, all RAE injected into the CA gap after the formation of potential hump are decelerated, which leads to efficient ionization and excitation of the N_2 gas. These electrons reach the anode with $\varepsilon_e < 10\,\text{keV}$ and one obtains a large spread of the EEDF and an increased time duration of the RAE beam. The results of the simulations showed that in this case the density of the generated plasma increases as compared with the case $|\varphi_C| = 10\,\text{kV}$ and $N_{max} = 10^6$ ($8.8 \times 10^{15}\,\text{cm}^{-3}$ versus $1.8 \times 10^{15}\,\text{cm}^{-3}$). However, the electric field in the vicinity of the cathode at $|\varphi_C| = 1.5\,\text{kV}$ is smaller than at $|\varphi_C| = 10\,\text{kV}$ and there is no streamer formation.

In addition, for $|\varphi_C| = 10\,\text{kV}$, $N_{max} = 10^7$, and $\tau = 100\,\text{ps}$, the simulations were carried out for $R_C = 300\,\mu\text{m}$ and $R_C = 3\,\mu\text{m}$ when the electric field in the vicinity of the cathode at $t = 0$ (beginning of the electron beam injection) is E_{cath} ($9.5 \times 10^4\,\text{V/cm}$) $< E_{cr}$ and E_{cath} ($4 \times 10^6\,\text{V/cm}$) $\gg E_{cr}$, respectively. It was obtained that at $R_C = 300\,\mu\text{m}$, the RAE breakdown develops qualitatively similarly to the case shown in Figs. 1(a) and 1(c) at $|\varphi_C| = 1.5\,\text{kV}$, $\tau = 70$ ps, $N_{max} = 10^6$, and $R_C = 3\,\mu\text{m}$. For the case $R_C = 300\,\mu\text{m}$, one obtains an increase in the duration of the RAE beam [compare Fig. 1(a) and Fig. 3(a)] and a wider spectrum of electrons at the anode [see Figs. 1(b) and 3(b)]. The wider spectrum is explained by the larger value of $|\varphi_C|$, and the increase in the duration of the RAE beam is caused by the deceleration of electrons from the beam tail in the electric field formed by the electrons from the head of the beam.

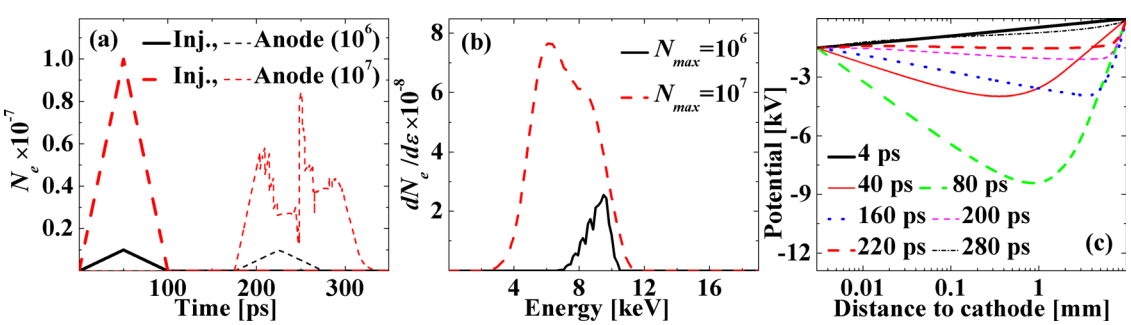

FIG. 2. (a) Comparison between RAE beam injected into the CA gap and RAE beam reaching the anode at $N_{max} = 10^6$ and $N_{max} = 10^7$ electrons; (b) electron energy distribution function at the anode at different amplitudes at $N_{max} = 10^6$ and $N_{max} = 10^7$ electrons; (c) potential distribution in the CA gap at different times at $N_{max} = 10^7$. $R_C = 3\,\mu\text{m}$, $\tau = 100\,\text{ps}$, and $|\varphi_C| = 1.5\,\text{kV}$.

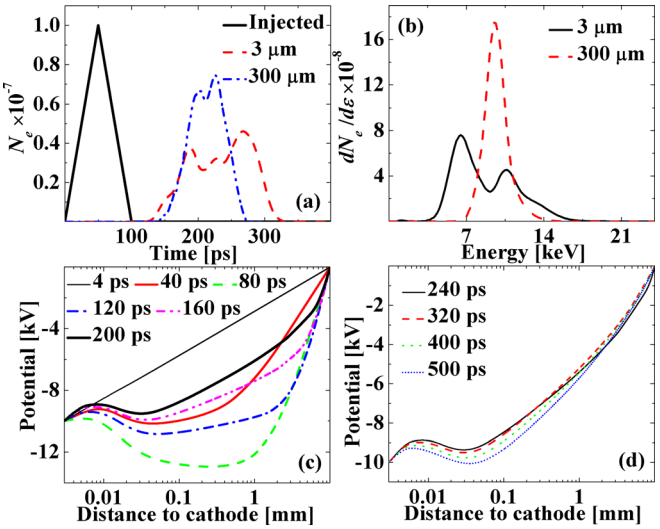

FIG. 3. (a) Comparison between RAE beam injected into the CA gap and RAE beam reaching the anode at a different radius of the cathode; (b) electron energy distribution function at the anode at a different radius of the cathode; (c) and (d) potential distribution in the CA gap at different times for the case $R_C = 3\ \mu$m. $N_{max} = 10^7$, $\tau = 100$ ps, and $|\varphi_C| = 10$ kV.

At $R_C = 3\ \mu$m, the RAE breakdown develops similarly to the cases presented in Figs. 1(d) and 2. Namely, one can see a significant time and energy spread of the RAE reaching the anode [see Figs. 3(a) and 3(b)]. In these conditions, the space charge of all the electrons inside the CA gap is large enough to disturb the external electric field [see Fig. 3(c)]. Fig. 3(c) shows that the potential inside the CA gap exceeds the cathode potential. However, the electric field from the anode side of this potential hump is much smaller than E_{cr} and RAE cannot be generated at that location. The formation of this hump is responsible for the obtained time and energy spread of the RAE beam shown in Figs. 3(a) and 3(b) for $R_C = 3\ \mu$m. The RAE beam propagating towards the anode is accompanied by a propagating FIW with a velocity of $\sim 1.4 \times 10^9$ cm/s, which is typical for high-voltage nanosecond discharges.[5–7,23] Behind the FIW, one obtains the plasma with $n_e \approx 8.1 \times 10^{15}$ cm^{-3}. Fig. 3(d) shows the potential distribution after the RAE beam has left the CA gap. In addition, the results of the simulations showed the formation of the streamer near the cathode propagating toward the anode with a velocity of $\sim 6 \times 10^6$ cm/s.

It is understood that one has to apply three-dimensional simulations to describe the streamer time and space evolution correctly. Nevertheless, the obtained velocity of the streamer agrees satisfactorily with published data.[21] However, this velocity is significantly smaller than the velocity one requires to explain the ~30 ps time interval between two peaks of RAE obtained in Ref. 3 and explained by the acceleration of electrons in the space between the anode and the boundary of the plasma approaching the anode. One can suppose that the electrons of the second peak of RAE are generated from the head of the propagating streamer with a small curvature radius and where electric field could exceed E_{cr}. In this case, the streamer must not be close to the anode.

IV. SUMMARY

The runaway breakdown initiated by the monoenergetic RAE beam was studied using the 1D PIC numerical model. It was shown that the parameters of the gaseous discharge depend on the initial conditions, namely, the number of the injected electrons and the potential difference between the cathode and anode. An increase in either the cathode potential or the amplitude of the RAE beam led to rather different discharge dynamics. If the space charge of the RAE becomes significant enough to cause a disturbance of the external electric field, but the total electric field in the vicinity of the cathode remains $>E_{cr}$, the amplitude of the RAE beam, leaving the gap, decreases with the increase in the duration of the beam. When the RAE beam has left the cathode-anode gap, one obtains the formation of the streamer near the cathode and its propagation toward the anode with a velocity of $\sim 10^7$ cm/s. When one increases the amplitude of the injected electrons or decreases the electric field, the space charge of the RAE changes the potential distribution in the vicinity of the cathode significantly, forming a potential hump, but there is no significant spread in the time and energy of the RAE leaving the CA gap. However, also in this case, streamer generation near the cathode is realized. Finally, the simulation results showed that, in spite the formation of rather dense plasma inside the CA gap by RAE, the electric field is not screened, which is explained by a large plasma resistivity because of frequent electron–neutral collisions.

ACKNOWLEDGMENTS

This work was supported in part at the Technion by a fellowship from the Lady Davis Foundation.

[1]A. V. Gurevich, G. A. Milikh, and R. Roussel-Dupre, Phys. Lett. A **165**, 463 (1992).
[2]A. V. Gurevich, K. F. Sergeichev, I. A. Sychov, R. Roussel-Dupre, and K. P. Zybin, Phys. Lett. A **260**, 269 (1999).
[3]A. V. Gurevich, G. A. Mesyats, K. P. Zybin, A. G. Reutova, V. G. Shpak, S. A. Shunailov, and M. I. Yalandin, Phys. Lett. A **375**, 2845 (2011).
[4]A. V. Gurevich and K. P. Zubin, Phys. Usp. **44**, 1119 (2001).
[5]L. P. Babich, T. V. Loiko, and V. A. Tsukerman, Phys. Usp. **33**, 521 (1990).
[6]V. F. Tarasenko and S. I. Yakovlenko, Phys. Usp. **47**, 887 (2004).
[7]D. Levko, Ya. E. Krasik, and V. F. Tarasenko, Int. Rev. Phys. **6**, 165 (2012).
[8]T. Shao, C. Zhang, Z. Niu, P. Yan, V. F. Tarasenko, E. Kh. Baksht, A. G. Burahenko, and Yu. V. Shutko, Appl. Phys. Lett. **98**, 021503 (2011).
[9]T. Shao, C. Zhang, Z. Niu, P. Yan, V. F. Tarasenko, E. Kh. Baksht, I. D. Kostyrya, and V. Shutko, J. Appl. Phys. **109**, 083306 (2011).
[10]T. Shao, V. F. Tarasenko, C. Zhang, M. I. Lomaev, D. A. Sorokin, P. Yan, A. V. Kozyrev, and E. Kh. Baksht, J. Appl. Phys. **111**, 023304 (2012).
[11]S. O. Macheret, M. N. Shneider, and R. B. Miles, IEEE Trans. Plasma Sci. **30**, 1301 (2002).
[12]G. A. Mesyats and M. I. Yalandin, IEEE Trans. Plasma Sci. **37**, 785 (2009).
[13]A. M. Boichenko, A. N. Tkachev, and S. I. Yakovlenko, JETP Lett. **78**, 709 (2003).
[14]A. N. Tkachev and S. I. Yakovlenko, JETP Lett. **77**, 221 (2003).
[15]V. A. Shklyaev and V. V. Ryzhov, Tech. Phys. Lett. **35**, 518 (2009).
[16]J. E. Chaparro, "Investigation of sub-nanosecond breakdown through experimental and computational methods," Ph.D. dissertation (Texas Tech University, 2008).
[17]D. Levko, S. Yatom, V. Vekselman, J. Z. Gleizer, V. Tz. Gurovich, and Ya. E. Krasik, J. Appl. Phys. **111**, 013303 (2012).

[18]I. M. Kutsyk, L. P. Babich, E. N. Donskoi, and E. I. Bochkov, JETP Lett. **95**, 631 (2012).
[19]Y. Itikawa, J. Phys. Chem. Ref. Data **35**, 31 (2006).
[20]G. D. Moss, V. P. Pasko, N. Liu, and G. Veronis, J. Geophys. Res. **111**, A02307, doi:10.1029/2005JA011350 (2006).
[21]Yu. P. Raizer, *Gas Discharge Physics* (Springer, Berlin, 1991).
[22]L. M. Vasilyak, S. V. Kostyuchenko, N. N. Kudryavtsev, and I. V. Filyugin, Phys. Usp. **37**, 247 (1994).
[23]D. Levko, V. Tz. Gurovich, and Ya. E. Krasik, J. Appl. Phys. **111**, 123303 (2012).